Retroreflective effect on a right angle left-handed media prism

Cesar Monzon,[1] Donald W. Forester,[2] and Richard Burkhart[2]
[1]*SFA Department NRL, Largo, Maryland 20774, USA*
[2]*Naval Research Laboratory, Washington, DC 20375, USA*
(Received 29 November 2005; published 24 March 2006)

A different retroreflective effect which parallels that encountered with dihedral corner reflectors is found in the scattering response of a penetrable left-handed media $\varepsilon=\mu=-1$ right angle prism. More significantly, no diffraction from the vertex is found to exist and hence no field singularity for the right angle wedge. Although the results are illustrated with microwaves, the concept finds applications in optics, acoustics, elasticity, and other media characterized by negative index wave propagation.

DOI: 10.1103/PhysRevE.73.036620 PACS number(s): 42.70.Qs, 41.20.−q, 42.25.−p, 42.79.−e

Diffraction problems involving planar surfaces are important aspects of electromagnetics, acoustics, elasticity, and optics; yet, exact rigorous solutions are quite rare. The first such rigorous solution corresponds to plane wave incidence on a perfectly electric conducting (PEC) half plane (a zero angle wedge), found by Sommerfeld over a century ago [1,2]. In the years that followed, incremental embellishments were made on the solution [3,4], and most importantly, generalization to a wedge by Bromwich [5]. Exact solutions for penetrable wedges are virtually nonexistent. The closest we can get to this is via equivalent impedance surfaces (impedance wedge) as done by Maliuzhinets [6] in a very elegant fashion.

Introduced by Veselago [7] 35 years ago as a hypothetical material where the phase velocity and energy flow in opposite directions, LHM is being implemented as a periodic array of elements a fraction of a wavelength in size [8–11]. As the discreteness in the material is reduced, a homogeneous material will result, enabling us to represent the periodic array via effective permittivity ε and permeability μ. Interest is centered in the ideal unit index left-handed media (LHM) case, as Pendry has proposed that it would allow a lens to perform an ideal reconstruction of an image. The problem of a wedge or angled prism is important, as it is the shape that has been employed consistently in measurements of LHM optical properties [8,12].

The object of this paper is to investigate the effect of the edge in the problem of plane diffraction by a right-handed unit index LHM wedge. In the process we find that under plane wave incidence the edge does not diffract at all, and that the main response of the wedge is a retroreflective effect akin to the dihedral reflector of scattering theory. Potential uses for such an object abound in optics and microwaves, as in certain applications it is desirable to enhance the reflection or radar return, as may be the case, for instance, of a moving object (aircraft or missile) being tracked from ground. Our device presents an alternative to the traditional corner reflector, but which can be made aerodynamic. Lack of edge diffraction on the other hand can be advantageous for applications involving bistatic signature modeling, including suppression.

We center our attention on materials for which $\varepsilon=\mu=-1+i\delta$, in the limit of very small losses $\delta\to 0$. The geometry is presented in Fig. 1, where the angle of incidence of the unit amplitude E polarized plane wave is θ_0 and the total wedge angle is 2α. Our main interest lies in the right angle case $\alpha=\pi/4$. The $e^{-i\omega t}$ time convention is assumed and suppressed throughout.

It has been found recently [13] that for arbitrary wedge angle α, and upon restricting the angle of incidence according to

$$3\alpha < \theta_0 < 2\pi - 3\alpha, \tag{1}$$

the total electric field is given by

$$E = \pi \sum_{n=0}^{\infty} e^{-i\nu\pi/2} J_\nu(k_0\rho) \times A_\nu^2 \begin{cases} \cos\{\nu[2\alpha - (\theta+\theta_0)]\}; & \theta \in (-\alpha,\alpha) \\ \cos[\nu(\theta-\theta_0)]; & \theta \in (\alpha, 2\pi-\alpha) \end{cases}. \tag{2}$$

This is the exact solution for the total electric field, for E-polarized unit amplitude plane wave incidence, and is valid everywhere in free space and in the LHM wedge. In the above,

$$\nu = n\pi/(\pi - 2\alpha), \quad A_\nu = \sqrt{\varepsilon_n/(\pi - 2\alpha)} \tag{3a}$$

and

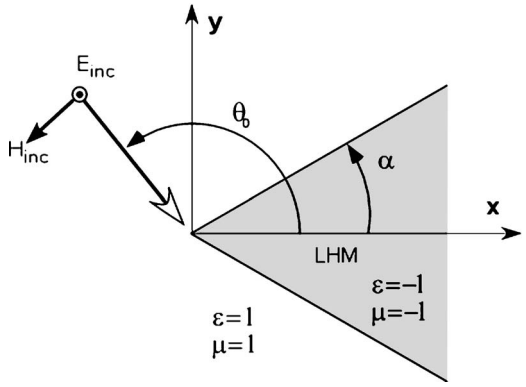

FIG. 1. Wedge geometry under plane wave incidence. For a right angle LHM wedge $\alpha=\pi/4$. The unit magnitude E-polarized plane wave is described by angle of incidence θ_0.

$$\varepsilon_n = \begin{cases} 1 & n = 0 \\ 2 & \text{otherwise} \end{cases}. \tag{3b}$$

For a right angle wedge, $\alpha \to \pi/4$, which results in $\nu \to 2n$, and the formula for the total electric field becomes

$$E = 2\sum_{n=0}^{\infty} \varepsilon_n J_{2n}(k_0\rho) \times \begin{cases} \cos[2n(\theta + \theta_0)]; & \theta \in (-\pi/4, \pi/4) \\ (-1)^n \cos[2n(\theta - \theta_0)]; & \theta \in (\pi/4, 7\pi/4) \end{cases} \tag{4}$$

which are Kapteyn series, where the top and bottom correspond to the interior and exterior fields. The above solution is exact everywhere.

It is important to mention that the E-polarization solution for a PEC wedge of total angle 2α is given by [14,15]

$$E = \frac{2\pi}{\pi - \alpha}\sum_{n=0}^{\infty} e^{-i\tau\pi/2} J_\tau(k_0\rho)\sin[\tau(\theta - \alpha)]\sin[\tau(\theta_0 - \alpha)] \tag{5}$$

for $\theta \in (\alpha, 2\pi - \alpha)$, and where the index $\tau = n\pi/2(\pi - \alpha)$ is to be compared with ν for the LHM wedge. For a PEC wedge of total angle $2\alpha = 3\pi/2$, τ becomes $2n$, just as in the case of ν. In view of the similarity of the expressions for the exterior region, the two solutions are expected to be comparable. The interesting thing is that such a PEC wedge is a corner reflector. Thus we should expect a very similar behavior from the right angled LHM prism in the free space region. The internal region is a different story.

By means of the following identity [16]:

$$J_0(z) + 2\sum_{n=1}^{\infty} J_{2n}(z)\cos(2n\beta) = \cos[z\sin(\beta)] \tag{6}$$

and using Eq. (3b) and the fact that $(-1)^n \cos[2n(\theta - \theta_0)] = \cos[2n(\theta - \theta_0 \pm \pi/2)]$, the exact solution Eq. (4) can be put in the form

$$E = \begin{cases} e^{ik_0\rho\cos(\theta - \theta_{LR})} + e^{ik_0\rho\cos(\theta - \theta_{RL})}; & \theta \in (-\pi/4, \pi/4) \\ e^{-ik_0\rho\cos(\theta - \theta_0)} + e^{ik_0\rho\cos(\theta - \theta_0)}; & \theta \in (\pi/4, 7\pi/4) \end{cases}, \tag{7}$$

where

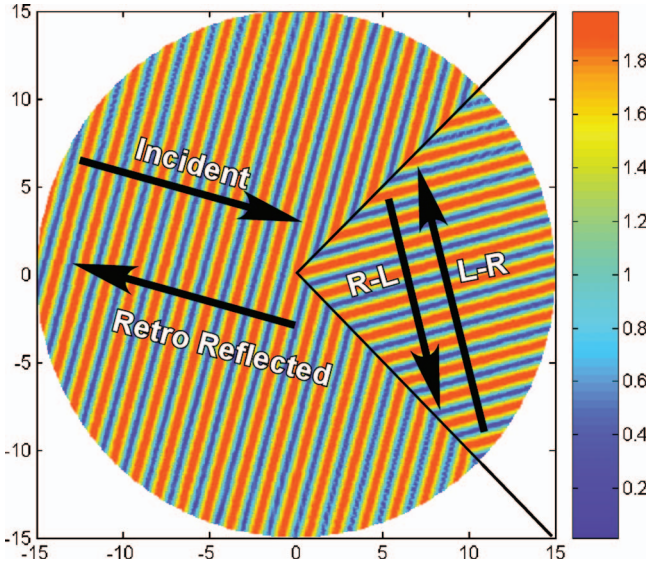

FIG. 2. (Color) Exact time-harmonic solution for a unit index LHM wedge for $\theta_0 = 165°$ at $\lambda = 3$ cm (all dimensions in cm). The colors depict the magnitude of the electric field, which varies from 0 to 2, indicating interfering waves of equal amplitude. The four waves correspond to the terms identified in Eq. (7), and result in continuous fields everywhere. Unlike ordinary media [14], there are no field singularities at the edge.

$$\theta_{LR} = \frac{3\pi}{2} - \theta_0, \quad \theta_{RL} = \frac{5\pi}{2} - \theta_0, \tag{8}$$

where θ_{LR} can be shown to be the angle of propagation of the refracted wave due to incidence on the lower wedge face (actually for arbitrary wedge angle $\theta_{LR} = \pi - \theta_0 + 2\alpha$). The subindex LR indicates that the wave travels from the left wedge face to the right face. Similarly, θ_{RL} is the angle of propagation of the refracted wave due to incidence on the top wedge face. The top of Eq. (7) indicates that in the material we only have two refracted waves, while the bottom says that outside the material we only have two waves, the incident field plus a wave that travels back in the direction of incidence, a retroreflected plane wave field. The four waves are illustrated in the time-harmonic interference pattern of Fig. 2, where the dimensions are in cm, $\lambda = 3$ cm, and $\theta_0 = 165°$. No edge diffracted fields are obtained therefore no field singularities at the edge.

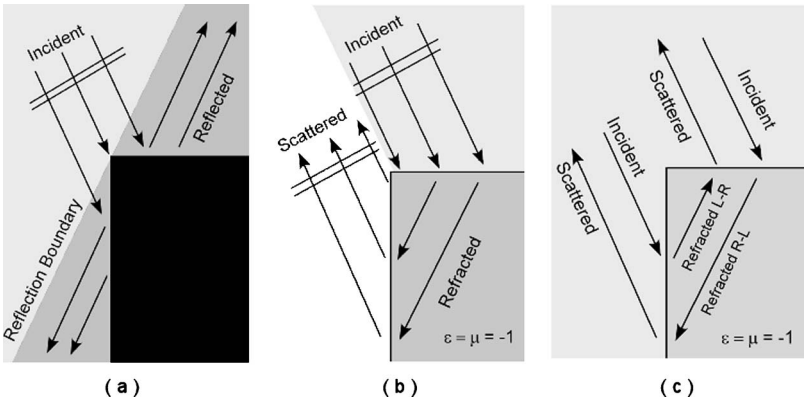

FIG. 3. Sketched GO solutions for PEC and LHM $\varepsilon = \mu = -1$ right angle wedges. The PEC case (a) leads to discontinuities at reflection boundaries necessitating an edge diffraction term to patch up the discontinuities. The LHM GO leads to discontinuities under single face illumination (b), but these disappear when both faces are illuminated (c); the end result being a single retroreflective scattered plane wave, and a standing wave inside the prism caused by the beating of the left-to-right (L-R) and right-to-left (R-L) refracted waves.

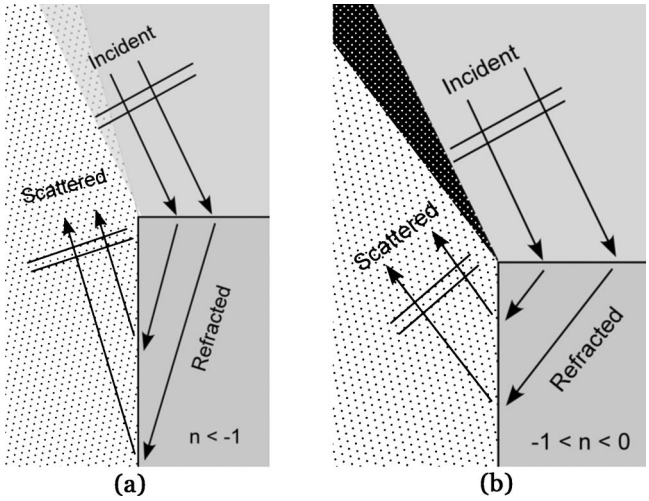

FIG. 4. Field discontinuities introduced in the free space region when the index is different from -1. (a) $n<-1$ where the two illuminated regions (incident and scattered) overlap; (b) $-1<n<0$ where the dark area is not illuminated. For convenience in the illustrations, only the top face of the prism is illuminated. Accounting for the illumination on both sides does not remove the discontinuities. Clearly an edge diffraction term is needed.

The physical reason for the absence of diffraction can be traced back to the asymptotic solution of diffraction canonical problems [14,15], where the diffraction terms always appear accompanying geometrical optics (GO) fields which are discontinuous, and which the diffraction terms help smooth out. The case of a metallic wedge is illustrated in Fig. 3(a), where only GO fields are depicted, illustrating that an edge diffraction term is needed to smooth out the discontinuities at the reflection boundaries. For the particular case at hand, LHM $\varepsilon=\mu=-1$, the GO solution for a right angle prism does not lead to discontinuous fields at reflection boundaries. For the case of single face illumination, the GO solution does contain discontinuities, as shown in Fig. 3(b), but these disappear when both faces are illuminated, as depicted in Fig. 3(c). The end result being a single retroreflective scattered plane wave in free space [just like a dihedral reflector, it happens for all angles of incidence that satisfy Eq. (1), i.e., $3\pi/4<\theta_0<5\pi/4$], and a standing wave inside the prism caused by the beating of the left-to-right (L-R) and right-to-left (R-L) refracted waves. Clearly, since the fields are already smooth everywhere; an edge diffraction term is not needed.

One may wonder if the same holds for an arbitrary index LHM right angle wedge. It can be readily shown through GO that for an index $n\neq-1$, there will be either dark or overlap regions in free space, with accompanying field discontinuities at the boundaries. This is depicted in Fig. 4, where for convenience, only the top face of the prism is illuminated, and where (a) results in an overlap for $n<-1$, and (b) shows a resulting dark region when $-1<n<0$. In both cases, edge diffraction is needed to eliminate the field discontinuities.

Similarly, if the index is $n=-1$, but the total wedge angle is not $\pi/2$, it can be shown that the GO scattered fields result in either dark or overlap regions, with accompanying field discontinuities at the boundaries. The effect is similar to that depicted in Fig. 4 for the right angle wedge, and will not be shown explicitly. Actually we can show through GO that providing Eq. (1) is satisfied, i.e., $3\pi/4<\theta_0<5\pi/4$, the scattered field corresponding to an incident angle θ_0 reemerges at an angle $\theta_S=\theta_0+\pi-4\alpha$, in other words, for unit index LHM, the retroreflected beam only occurs for a right angle prism. Hence we conclude that when the index $n=-1$, but the total wedge angle is not $\pi/2$, there will be no retroreflective field, but there will be an edge diffracted field.

For verification purposes we used MAXTDA [17], a finite difference time domain (FDTD) code which employs rectangular cells. MAXTDA's model of the 90° wedge ($\alpha=45°$) is made conformal with the x-y plane to avoid surface roughness in the model. The scatterer is a square 10 wavelength on the side with a 10-GHz carrier plane wave radar pulse of incidence angle $\theta_0=165°$. We assume a strongly dispersive Lorentzian medium characterized by $\varepsilon(f)=\mu(f)=1+(K-1)/\{1-i(fG/f_o^2)-(f/f_o)^2\}$. Using $G=0.04$ GHz, $K=4.0$, and $f_o=6.3$ GHz, the index becomes negative around 10 GHz, $n(10\text{ GHz})=-1.001+i0.013$, resulting in LHM behavior. Figure 5 shows the geometry, and an FDTD snapshot of the electric field magnitude after the time-harmonic steady state has been established for the lower left edge (at 80 periods). Clearly there is no diffracted field, and the local left-lower wedge solution is incident plus retroreflected (outside) with a standing wave between the two refracted (inside). The high level of interference indicates that both waves are of the same magnitude, just as expected from the exact wedge solution (away from the left-lower edge we observe the influence of the finiteness of the object, and this region should be disregarded). We conclude that the local wedge exact and FDTD solutions are essentially identical and that the small deviation from ideal lossless conditions is not meaningful within the range of distances encountered.

If the above interpretation is correct, an electrically large but finite square could have a ray path where the energy will just be guided (in a duct, from incident to refracted and then transmitted), and another (reduced) region with a standing wave resulting in a retroreflected field of less than optimal amplitude. This is illustrated in Fig. 6 (left) which shows the nature of the expected ray solution on a LHM square of 20 wavelengths on a side, where material and incidence is the same as that of the previous example. A snapshot of the magnitude of the FDTD time-harmonic electric field is presented in Fig. 6 (right), where all the different regions sketched by the ray picture are validated (black lines were introduced to clarify the regions). The lighter amplitude seen at the lower-left edge is due to a time delay (at other times that edge and its neighborhood flares up), and does not imply diffraction. The internal lower triangular section is clearly the interference between the two refracted waves, whereas the region between the two skewed lines is the duct, where the amplitude is not as large indicating an eminently single propagating wave region (this is not a standing wave, we are plotting the electrical field magnitude at a given time). The shadow region is also evident in the figure. Departure from the ray picture is significant only in the neighborhood of the other edges, where our assumptions break down.

This 20λ LHM square has been further analyzed under bistatic conditions using a GO approximation, neglecting

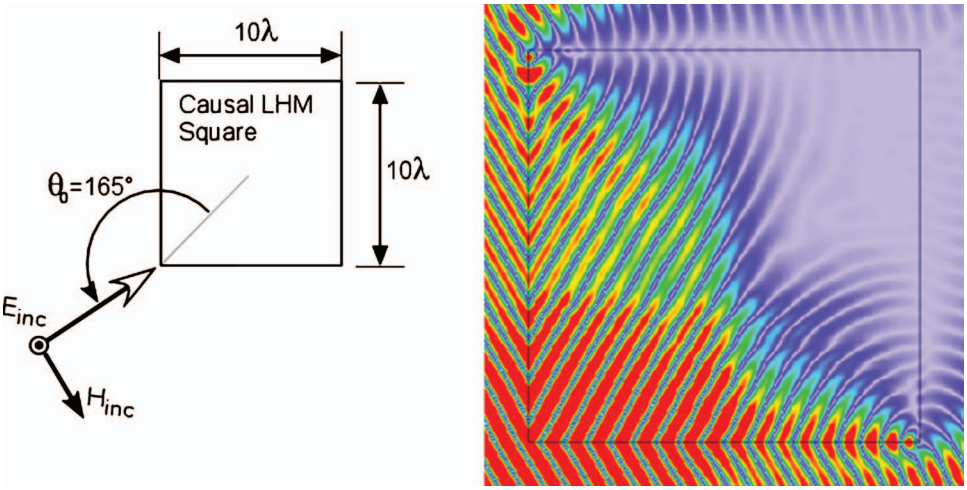

FIG. 5. (Color) Exact FDTD time-harmonic solution for a slightly lossy and causal LHM square cylinder 10λ on a side at 10 GHz (index $n=-1.001+i0.013$). The sketch on the left shows the geometry. The color plot illustrates time-domain electric field magnitudes (data obtained after 80 periods have passed). $\lambda=3$ cm, $\alpha=45°$, $\theta_0=165°$. The front edge fields are identical to those observed in Fig. 2 therefore validating Eq. (7).

losses, and assuming that the RCS is equal to the projected area of the region responsible for the retroreflected beam (region sketched in Fig. 6). For L the side of the square, and for the angle of incidence defined as in Fig. 1 or Fig. 5, it can be shown that the two-dimensional (2D) monostatic RCS in the absence of losses is given by

$$\sigma_{MONO}=2L\sin(\theta_0-3\pi/4). \tag{9}$$

Although the material is impedance matched to free space for normal incidence, any deviation from an ideal index $n=-1.00$ will induce reflections under oblique incidence [15]. This means that a small part of the two refracted waves will undergo an extra reflection and refraction before exiting the scatterer, causing two small bistatic beams aligned with θ_{LR} and θ_{RL} to be formed. The details are implicit in the sketch of Fig. 7, which also details the FDTD bistatic calculation at 10 GHz. Finally, it should be mentioned that bistatic scattering in the forward direction is the unusual composition of the ordinary "shadow" (or $-E^{\text{inc}}$ field) and the duct transmitted field, resulting in a significant beam. The agreement with the beam location is excellent. On the other hand, in the backward direction $\theta=165°$, and for $L=20\lambda$, $\sigma_{MONO}/\lambda=20$ (13 dB), and a 6-dB difference is observed between Eq. (9) and the simulation, and explained as due to the losses (the refracted paths lengths are dissimilar and electrically very long) which not only reduces the effective aperture, but also damage the retroreflected phase front leading to a wider scattered beam. Other simulations (not shown) for smaller losses show a narrowed and larger amplitude beam that approaches Eq. (9).

The results presented are also applicable to H-polarized plane wave incidence. This extension comes from recognizing that the LHM wedge is self-dual, and that under duality [14], $E\rightarrow H$, $H\rightarrow -E$, and $\mu\leftrightarrow\varepsilon$. Hence application of duality to the present configuration translates directly into the H-polarization problem. This means that a unit index LHM cylinder of square cross section can act as a monostatic reflector whose efficiency depends on the amount of loss in the material. Extension of this lens to three dimensions is possible, in the shape of a toroid of square cross section (comparable to a biconical reflector [15]). Applications for radar reflectors abound.

It should be mentioned that in a metamaterial realization of the unit index LHM wedge [8–10,12,18], the unit-cell size must be much smaller than the free space wavelength, so that the material could be expected to be reasonably well characterized by effective medium theory. A finite cell size, however, usually leads to stepping of the surface. It is known that when the cell size is a significant fraction of the wavelength, the imperfect surface act like a grating [19]; the resulting diffraction having a detrimental effect on the LHM performance. This may not be the case in our right angle prism if

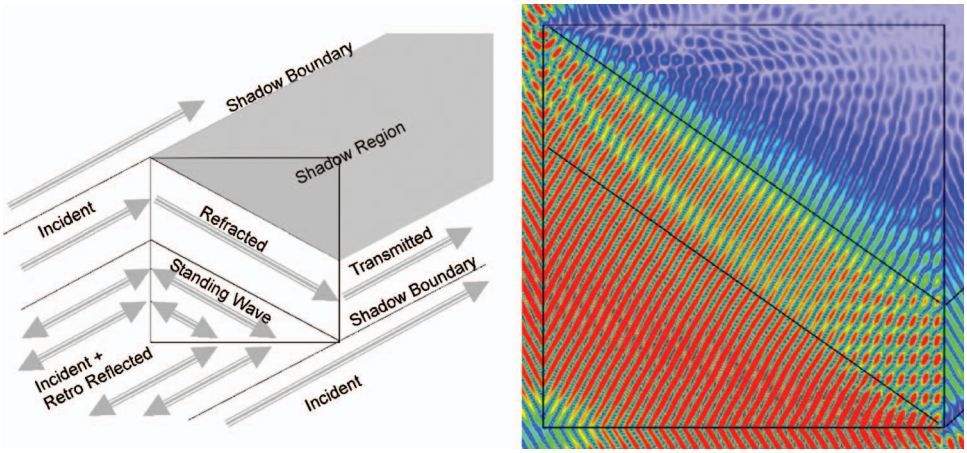

FIG. 6. (Color) Exact FDTD time-harmonic solution for a slightly lossy LHM square cylinder 20λ on a side at 10 GHz (index $n=-1.001+i0.013$). The sketch on the left shows the ray contributions expected from Eq. (7). The color plot shows time-domain electric field magnitude (after 200 periods have passed). $\lambda=3$ cm, $\alpha=45°$, $\theta_0=165°$. All expected features are observed clearly therefore validating Eq. (7).

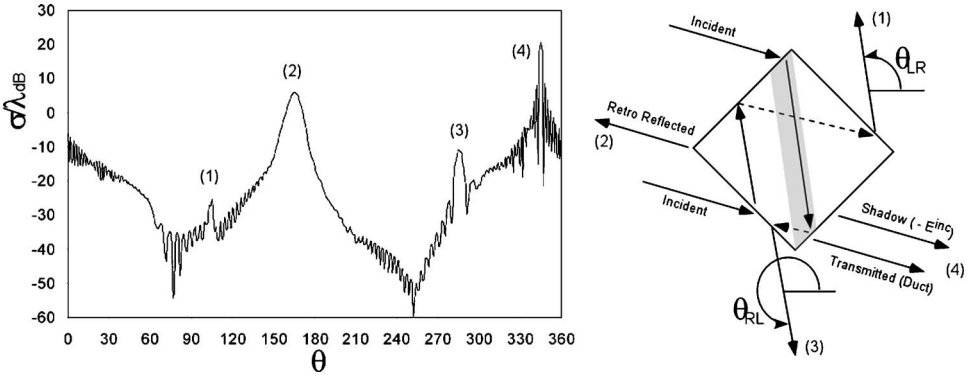

FIG. 7. Bistatic RCS for a lossy $n=-1.001+i0.013$ square cylinder 20λ on a side. *E* polarization, FDTD, λ=3 cm, $\alpha=45°$, $\theta_0=165°$. The sketch on the right depicts the expected four main scattered beams, and their location is shown in the bistatic plot. The retroreflected beam peak, identified as (2), is lower than predicted by Eq. (9) due to the loss and the long lengths of the refracted paths.

the material lattice is square and conformal with the prism (no stepping of the surface), with an electrically small cell size. Further, since for effective theory to hold we need to average over a number of cells, we expect an edge "singularity" at the very edge, up to distances comparable to a cell size. This based on electrostatics, and provided a dielectric binder other than low index foam is employed, as otherwise, no singularity is expected.

To summarize, no diffraction from the vertex and no edge field singularity are found to exist for the unit index LHM right angle wedge. A different retroreflective effect which parallels that encountered with dihedral reflectors is identified turning the scatterer into a different type of monostatic enhancement lens. The results are verified by comparison with numerical simulations on finite, causal LHM scatterers.

[1] A. Sommerfeld, Math. Ann. **47**, 317 (1896).
[2] A. Sommerfeld, *Optics* (Academic Press, New York, 1952).
[3] H. S. Carslaw, Proc. London Math. Soc. **30**, 121 (1899).
[4] H. M. MacDonald, *Electric Waves* (Cambridge University Press, Cambridge, England, 1902).
[5] T. J. I. A. Bromwich, Proc. London Math. Soc. **14**, 450 (1916).
[6] G. D. Maliuzhinets, Sov. Phys. Dokl. **3**, 752 (1958).
[7] V. G. Veselago, Sov. Phys. Usp. **10**, 509 (1968).
[8] R. A. Shelby *et al.*, Science **292**, 77 (2001).
[9] D. R. Smith *et al.*, Phys. Rev. Lett. **84**, 4184 (2000).
[10] R. A. Shelby *et al.*, Appl. Phys. Lett. **78**, 489 (2001).
[11] F. J. Rachford *et al.*, Phys. Rev. E **66**, 036613 (2002).
[12] A. A. Houck *et al.*, Phys. Rev. Lett. **90**, 137401 (2003).
[13] C. Monzon *et al.*, Phys. Rev. E **72**, 056606 (2005).
[14] D. S. Jones, *The Theory of Electromagnetism* (MacMillan, New York, 1964).
[15] *Radar Cross Section Handbook*, edited by G. T. Ruck (Plenum Press, New York, 1970).
[16] I. S. Gradshteyn and I. M. Ryzhik, *Table of Integrals, Series, and Products* (Academic, New York, 1980).
[17] MAXTDA, written at GTRI, includes causal forms for permittivity and permeability.
[18] C. Monzon and D. W. Forester, Phys. Rev. Lett. **95**, 123904 (2005).
[19] D. R. Smith *et al.*, Phys. Rev. Lett. **93**, 137405 (2004).